

ARTICLE IN PRESS

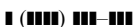
Available online at www.sciencedirect.com



1
3 ELSEVIER



Journal of the Mechanics and Physics of Solids



JOURNAL OF THE
MECHANICS AND
PHYSICS OF SOLIDS

www.elsevier.com/locate/jmps

5
7
9 On the possibility of piezoelectric nanocomposites
11 without using piezoelectric materials

13 N.D. Sharma, R. Maranganti, P. Sharma*

15 *Department of Mechanical Engineering, University of Houston, Houston, TX 77204, USA*

17 Received 11 December 2006; received in revised form 25 March 2007; accepted 28 March 2007

19 **Abstract**

21 In this work, predicated on nanoscale size-effects, we explore the tantalizing possibility of creating
23 apparently piezoelectric composites without using piezoelectric constituent materials. In a
25 piezoelectric material an applied *uniform* strain can induce an electric polarization (or vice-versa).
27 Crystallographic considerations restrict this technologically important property to non-centrosym-
29 metric systems. *Non-uniform strain* can break the inversion symmetry and induce polarization even in
31 non-piezoelectric dielectrics. The key concept is that *all* dielectrics (including non-piezoelectric ones)
33 exhibit the aforementioned coupling between strain gradient and polarization—an experimentally
35 verified phenomenon known in some circles as the flexoelectric effect. This flexoelectric coupling,
37 however, is generally very small and evades experimental detection unless very large strain gradients
(or conversely polarization gradients) are present. Based on a field theoretic framework and the
associated Greens function solutions developed in prior work, we quantitatively demonstrate the
possibility of “designing piezoelectricity,” i.e. we exploit the large strain gradients present in the
interior of composites containing nanoscale inhomogeneities to achieve an overall non-zero
polarization even under an uniformly applied stress. We prove that the aforementioned effect may be
realized only if both the shapes and distributions of the inhomogeneities are non-centrosymmetric.
Our un-optimized quantitative results, based on limited material data and restrictive assumptions on
inhomogeneity shape and distribution, indicate that apparent piezoelectric behavior close to 10% of
Quartz may be achievable for inhomogeneity sizes in the 4 nm range. In future works, it is not

43 *Corresponding author. Tel.: +1 713 743 4256.
45 *E-mail address:* psharma@uh.edu (P. Sharma).

1 unreasonable to expect enhanced performance based on optimization of shape, topology and
 appropriate material selection.

3 © 2007 Published by Elsevier Ltd.

5 Keywords: ■; ■; ■

7

1. Introduction and central concept

9

11 Non-centrosymmetry is a necessary condition for a crystal to exhibit piezoelectricity,
 where an applied *uniform* strain induces electric polarization (or vice versa). Here the
 polarization vector \mathbf{P} is related to the second-order strain tensor $\boldsymbol{\varepsilon}$ through the third-order
 13 piezoelectric tensor \mathbf{p}

$$15 \quad P_i = p_{ijk} \varepsilon_{jk}. \quad (1)$$

17 Tensor transformation properties require that under inversion-center symmetry, all odd-
 order tensors vanish. Thus, most common materials, e.g. Silicon, and NaCl are not
 piezoelectric whereas ZnO and GaAs are. The simple schematic in Fig. 1 illustrates the
 19 molecular origins of the classical piezoelectric effect. However, it is possible to visualize
 how a *non-uniform strain* or the presence of *strain gradients* may potentially break the
 21 inversion symmetry and induce polarization even in *centrosymmetric* crystals (Fig. 2).
 Formally, this is tantamount to extending Eq. (1) to include strain gradients

23

$$25 \quad P_i = \underbrace{p_{ijk} \varepsilon_{jk}}_{=0, \text{ for non-piezo materials}} + \mu_{ijkl} \frac{\partial \varepsilon_{jk}}{\partial x_l}. \quad (2)$$

27 Here μ_{ijkl} are the so-called flexoelectric coefficients. Although the components of the
 third-ordered tensor ' \mathbf{p} ' (piezoelectric coefficients) are non-zero for only selected
 29 (piezoelectric) dielectrics, the flexoelectric coefficients (components of the fourth-order
 tensor ' $\boldsymbol{\mu}$ ') are non-zero for all dielectrics. This implies that under a non-uniform strain, at

31

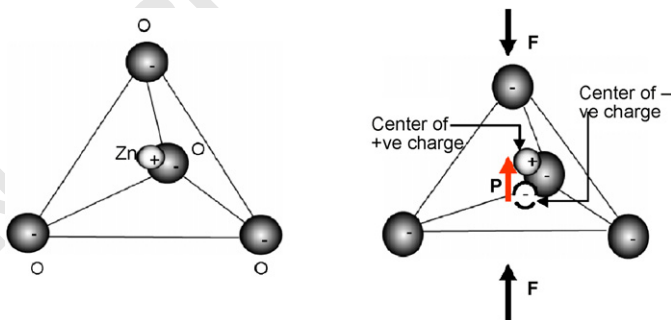
33

35

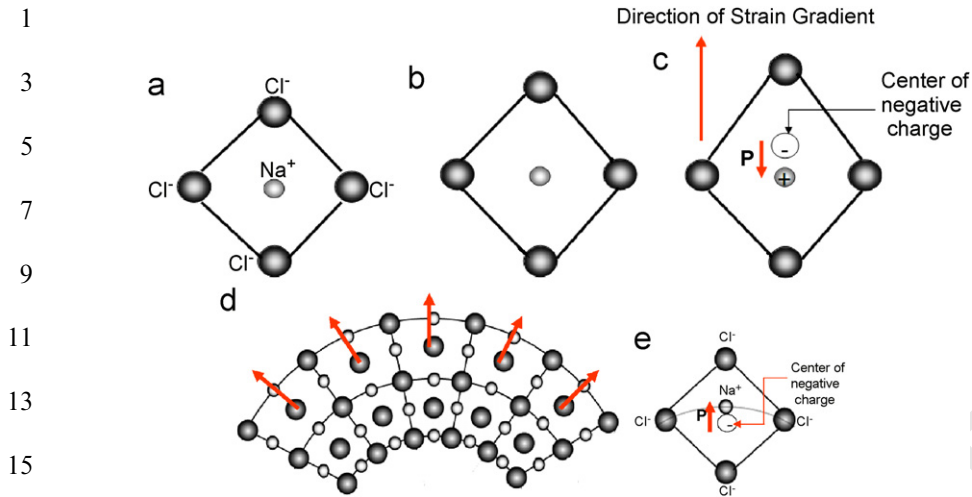
37

39

41



43 Fig. 1. Illustration of "Classical" piezoelectricity. The left figure shows the tetrahedrally coordinated
 cation-anion unit of a ZnO crystal. The center of negative charge of the oxygen (O) anions coincides with the
 45 center of positive charge, which is located at the Zinc (Zn) ion. Thus, there is no net dipole polarization in the
 absence of external pressure. Upon application of external pressure, the centers of positive and negative charge
 suffer relative displacement with respect to each other thereby inducing a dipole moment. Such dipole moments
 47 are induced throughout the crystal lattice thereby giving rise to net polarization.



17 Fig. 2. (a) Undeformed NaCl unit cell. The sodium ion is positively charged while the four neighboring chlorine
 19 ions are negatively charged. As can be seen, the center of gravities of the negative charge and the positive charge
 21 coincide leading to (expectedly) zero net dipole moment. (b) Uniform Strain: application of a uniform strain
 23 displaces the identical ions equally from the center of inversion and hence the centers of the negative and positive
 25 charges coincide again thereby resulting in zero net polarization implying that NaCl is non-piezoelectric. (c) NaCl
 27 unit cell under non-uniform stretching. Application of a non-uniform strain however results in relative
 29 displacement of the centers of the negative charge and positive charge with respect to each other. This results in a
 31 dipole moment (represented by the thick red arrow) in the direction opposite to the strain gradient for the
 33 considered cell. (d) and (e) Polarization due to bending.

35 least in principle, all dielectric materials are capable of producing a polarization. The
 37 reader is referred to our recent work (Maranganti et al., 2006) that discusses flexoelectricity
 39 in detail although essential concepts are summarized here as well.

41 The universal strain gradient—polarization coupling can be interpreted from the point
 43 of view of two length scales: (i) at the length scale of a single (or few) unit cell(s), (ii) at a
 45 coarser length spanning many individual crystalline unit cells, i.e. the dimension of a
 47 nanostructure or larger. At the unit cell level, Fig. 2 illustrates how NaCl (which is non-
 piezoelectric) will yield zero net dipole moment (and hence no polarization) under
 application of uniform strain but will exhibit an apparent piezoelectric effect when
 subjected to strain gradients, e.g. bending or inhomogeneous stretching. At a coarser
 length scale, the effect of individual unit cells is accounted for in the phenomenologically
 introduced flexoelectric coefficients (Eq. (2)). As long as the flexoelectric coefficients are
 non-negligible, a finite polarization will manifest at coarser scales provided the
 nanostructures are properly designed. By proper design, we imply that the overall
 symmetry of the nanostructure must be such that the average of the polarization due to the
 presence of strain gradients is non-zero. For example, a heterogeneous spherical particle
 consisting of two different non-piezoelectric materials when subjected to uniform stress
 will exhibit spatially varying polarization due to flexoelectricity. The polarization will be
 significant if the particle is in the nanoscale size and if the difference in the dielectric and
 elastic properties of the constituents is large since the strain gradients will then be large.
 However, symmetry indicates that the net average polarization will regardless be zero.

1 Thus, “proper design” in the present context refers to (i) optimum topology, (ii) optimum
 differences in the material properties of the constituents that comprise the nanostructures,
 3 and (iii) optimum size.

Fig. 3 illustrates the main principle from a coarse-grained perspective.

5 Consider a composite consisting of two or more different non-piezoelectric dielectric
 materials. Even under application of uniform stress, a non-uniform strain distribution will
 7 be generated in this system. Due to the presence of strain gradients and the flexoelectric
 coupling, polarization will ensue. For “properly designed” nanocomposites, the net
 9 average polarization will be non-zero. Thus, the nanostructure will exhibit an overall
 electromechanical coupling under uniform stress behaving like an “apparently” piezo-
 11 electric material. The individual constituents must be at the nanoscale since this concept
 requires very large strain gradients and those (for a given strain) are generated easily only
 13 for small-scale structures (Fig. 4).

Both mathematically (Eq. (2)) and physically (Figs. 2 and 3), it is *manifestly possible* to
 15 induce electric fields in non-piezoelectrics via strain gradients. The next logical question is
 how significant is this effect? As will be quantitatively demonstrated in later section, this
 17 effect is of appreciable amount (for most dielectric materials) only at the nanoscale and
 thus is most relevant in the context of nanostructures. Due to the role of gradients,
 19 flexoelectricity is essentially a size-effect and negligible at supra-nano length scales (for

21

23

25

27

29

31

33

35

37

39

41

43

45

47

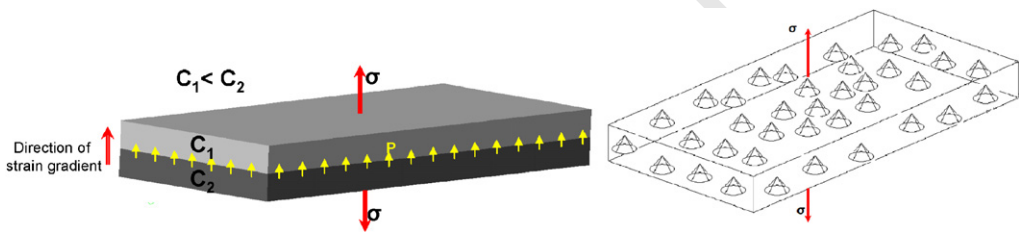


Fig. 3. Through suitable topology, arrangement, constituent property difference and selection of optimum size, heterogeneous nanostructures (i.e. bi-laminate or film with conical inclusions) such as shown in the figure can be created that will yield an “apparently” piezoelectric behavior despite the constituents being non-piezoelectric. Here C_1 and C_2 denote the ‘elastic constants’ of the two materials considered. The second figure is adapted from paper by Cross and co-workers (Fousek, et al., 1999, Cross, 2006)

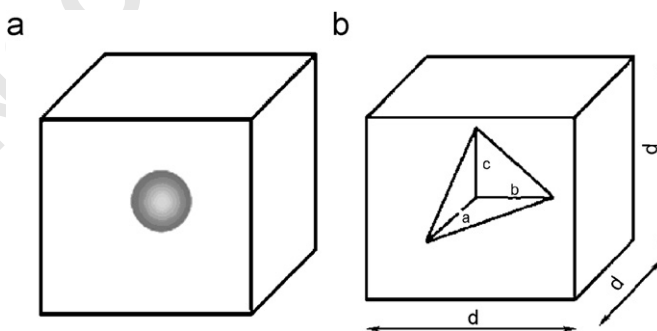


Fig. 4. Embedded inclusions (a) centrosymmetric (spherical) inclusion (b) non-centrosymmetric (orthogonal polyhedral) inclusion.

1 most ordinary dielectrics). Consider a structure with certain mechanical boundary
 conditions; the mechanical strain can be considered to be roughly the same if the system is
 3 shrunk self-similarly from mm's to nm's. However, the strain *gradient* will increase by six
 orders of magnitude! Incidentally, the statement regarding size-independence of strain is
 5 not *strictly* true (e.g. Zhang and Sharma, 2005a, b, Sharma et al., 2003); there is a size-
 dependency to strain at the nanoscale but that does not influence the point we are trying to
 7 make here, i.e. even if strain were size-independent, the strain gradient scales inversely with
 size. Flexoelectric coefficients are not readily available but some reasonable estimates are
 9 known for graphene (Dumitrica et al., 2002) and NaCl (Askar and Lee, 1974). Choosing
 the latter as an example, we can calculate its electromechanical coupling coefficient under
 11 applied voltage. One would expect it to be zero since NaCl is non-piezoelectric. However, if
 the flexoelectric effect is properly taken into account, it can be inferred that at 10 nm
 13 thickness, the electromechanical coupling factor reaches 80% of the value of Quartz or
 alternatively 12% of lead zirconate titanate (PZT) (Mindlin, 1968).

15 The flexoelectric phenomenon has been experimentally observed during bending of
 crystal plates (e.g. Bursian and Trunov, 1974) and measurements on thin films (Catalan et
 17 al., 2004). Mindlin (1968) used the converse of the flexoelectric effect to explain the
 anomalous capacitance measurements of thin dielectric films while Yakobson and
 19 coworkers employed it to discuss the polarization in curved carbon shells (Dumitrica et
 al., 2002). Experiments with dislocated non-piezoelectric dielectric crystals have attributed
 21 overall electromechanical coupling to polarization in the vicinities of dislocations (e.g.
 Whitworth, 1964; Nowick and Heller, 1965; Bauer and Brantley, 1970; Robinson et al.,
 23 1978).¹ The flexoelectric effect may also be used to provide an explanation for the size-
 dependent piezoelectric behavior of boron nitride nanotubes (Nakhmanson et al., 2003).
 25 The aforementioned works are related to crystalline materials. As an aside, we note here
 that a large literature also exists in the liquid crystal and biological membrane context. It is
 27 noteworthy though that the term, “flexoelectricity” for crystalline materials was coined
 inspired by similar phenomenon in liquid crystals (Meyer, 1969; Schmidt et al., 1972;
 29 Indenbom et al., 1981).

Kogan (1963) has argued that for all dielectrics, e/a ($\approx 10^{-9}$ C/m) is an appropriate
 31 lower bound for the flexoelectric coefficients, where e is the electronic charge and a is the
 lattice parameter. Later experiments (Ma and Cross, 2001a) and simple linear chain
 33 models of ions (Marvan and Havranek, 1997) suggested multiplication by relative
 permittivity for normal dielectrics. Much larger magnitudes ($\approx 10^{-6}$ C/m) of flexoelectric
 35 coefficients than this lower bound are observed in certain ceramics (Ma and Cross, 2001b,
 2002, 2003). Electric field created in non-piezoelectric CaWO_4 crystals with 4/m symmetry
 37 by applying a twisting moment was experimentally measured by Zheludev et al. (1969),
 which though closely related to flexoelectricity, was attributed mainly to disappearance of
 39 centrosymmetry due to applied torsion. Marvan and Havranek (1988) found presence of
 flexoelectric effect in an isotropic elastomer with flexoelectric coefficients roughly of the
 41 order of e/a . Flexoelectricity, of course also exists in materials that are already piezoelectric
 and in fact experimental evidence suggests that flexoelectric coefficients are unusually high
 43 in such materials—see the experimental work of Cross and co-workers (2001a, b, 2002,
 2003, 2006) on ferroelectric perovskites like PMN, PZT, and BST. In fact, the notion of
 45

47 ¹For this to occur, a necessary requirement is that the crystalline solid contain an excess of dislocation of a
 certain sign.

1 creating “apparently piezoelectric” composites without using piezoelectric constituents
 2 appears to have first appeared in a work by Fousek et al. (1999) and more recently in work
 3 by Zhu et al. (2006) who have experimentally realized this concept.²

4 Lattice level “shell” type models of crystalline dielectrics clearly indicate that the long
 5 wavelength limit of the lattice dynamical results do not lead to the classical piezoelectric
 6 theory, which from an atomistic point of view, is simply the long wavelength
 7 representation of the core–core interactions while core–shell and shell–shell interactions
 8 are neglected (Cochran and Cowley, 1962; Dick and Overhauser, 1958; Tolpygo, 1962). To
 9 tackle this discrepancy, Mindlin (1968) introduced a continuum field theory that
 10 incorporates coupling of polarization gradients to strain (or in our language—the
 11 converse flexoelectric effect). This theory is found to correctly represent the core–shell and
 12 shell–shell interactions within a continuum field-theoretic formalism (see also the study of
 13 Askar and Lee, 1974). It should be noted that Mindlin’s theory does not incorporate the
 14 direct flexoelectric effect or the strain gradient–polarization coupling discussed earlier.
 15 Several work subsequently expanded on Mindlin’s original theory. Askar et al. (1971)
 16 considered elastic and dielectric state of cylindrical and spherical cavities as well as cracks.
 17 In a later paper, using lattice dynamical methods, the same authors also evaluated the
 18 material constants of Mindlin’s theory for KCl and NaCl (1974). From the view-point of
 19 condensed matter physics, Tagantsev (1986, 1991) has proposed a phenomenological
 20 description and, in addition to providing a review, clarified several concepts related to both
 21 flexoelectricity and piezoelectricity based upon microscopic considerations.

22 Yet another electromechanical coupling effect which deserves mention is the well-known
 23 phenomena of electrostriction (Maugin, 1988) which is also universal for dielectrics.
 24 Electrostriction is a nonlinear effect and becomes operative at very high electric fields—the
 25 developed strain depends on the square of the electric field and consequently the direction
 26 of the electric field is independent of the sign of the strain (compression versus tension). In
 27 addition, an inverse electrostriction effect does not exist, i.e. deformation does not produce
 28 an electric field. This nonlinear effect is ignored in the present work since we only consider
 29 linearized theories and thus small strains (although not small *strain gradients*).

30 In the present work, based on a field theoretic framework and the associated Greens
 31 function solutions developed in prior work (Maranganti et al., 2006), we quantitatively
 32 demonstrate the possibility of “designing piezoelectricity,” i.e. we exploit the large strain
 33 gradients present in the interior of composites containing nanoscale inhomogeneities to
 34 achieve an overall non-zero polarization even under applied uniform stress. We show that
 35 the governing equations for flexoelectricity demand that the inhomogeneity shape must be
 36 non-centrosymmetric for a non-zero average polarization.

37 The paper is organized as follows. In Section 2, we discuss the mathematical framework
 38 and the governing equations for the extended theory of electromechanical coupling. In
 39 Section 3, we develop solutions for the embedded inclusion problem subject to dilatational
 40 transformation strain. Centrosymmetric (spherical) and non-centrosymmetric (orthogonal
 41 polyhedral) shapes are used to demonstrate that to obtain non-zero average polarization in
 42 the aforementioned “meta material”, the requirement of material non-centrosymmetry is
 43 transferred to requirement of shape non-symmetry of the inhomogeneity and topology
 44 arrangement. In Section 4, we propose a simple proof of this proposition. The

45
 46 ²This was brought to our attention by one of the anonymous referee’s at an advanced stage of the peer-review
 47 process.

1 homogenization scheme used to obtain quantitative results is discussed in Section 5 while
 2 the numerical calculations are presented in Section 6. We conclude in Section 7.

5 2. Mathematical framework and governing equations

7 Assuming an isotropic centrosymmetric³ dielectric, the most general expression for the
 8 linearized internal energy density function Σ incorporating terms involving first gradients
 9 of the deformation gradient and the polarization is (Sahin and Dost, 1988)

$$11 \quad \Sigma = \frac{1}{2}a_{kl}P_kP_l + \frac{1}{2}b_{ijkl}P_{i,j}P_{k,l} + \frac{1}{2}c_{ijkl}\varepsilon_{ij}\varepsilon_{kl} + d_{ijkl}P_{i,j}\varepsilon_{kl} + f_{ijkl}P_iu_{j,kl} + \frac{1}{2}g_{ijklmn}u_{i,jk}u_{l,mn} \quad (3)$$

13 \mathbf{u} and \mathbf{P} being displacement and polarization vectors respectively, ε_{ij} are the components of
 14 the infinitesimal strain tensor $\boldsymbol{\varepsilon}$ defined as

$$15 \quad \varepsilon_{ij} = \frac{1}{2}(u_{i,j} + u_{j,i}). \quad (4)$$

17 Unless stated otherwise, Cartesian basis is used throughout and both index and direct
 18 notation will be used as convenient. ‘ \mathbf{a} ’ is second-order reciprocal dielectric susceptibility,
 19 ‘ \mathbf{c} ’ is fourth-order elastic constant tensor, ‘ \mathbf{d} ’ is the tensor corresponding to higher-order
 20 electro-elastic couplings which link gradients of polarization to strains, ‘ \mathbf{b} ’ is the tensor
 21 corresponding to the converse flexoelectric effect and is thus coupled to polarization
 22 gradients, ‘ \mathbf{f} ’ is the tensor of flexoelectric coefficients, while ‘ \mathbf{g} ’ dictates purely elastic
 23 nonlocal effects corresponding to the strain gradient elasticity theories. The extended
 24 theory implicit in Eq. (3) differs from classical theory of piezoelectricity in that
 25 characteristic length scales appear and (as expected and desired) results are size-dependent.
 26 Such formalism is a modified version of Mindlin’s framework (Mindlin, 1968) and has
 27 been further developed in our earlier work (Maranganti et al., 2006).

28 Neglecting the purely elastic nonlocal effects (i.e. ‘ \mathbf{g} ’) for an isotropic continuum
 29 occupying domain Ω and boundary S , standard variational analysis of Eq. (3) can be used
 30 to obtain the following system of equilibrium equations, boundary conditions and
 31 constitutive relations:

32 *Equilibrium equations:*

$$33 \quad (t_{ij} - t_{jlm,m})_j + F_i = 0, \\
 34 \quad E_{ij,j} + E_i - \phi_{,i} + E_i^0 = 0, \\
 35 \quad -\varepsilon_0\phi_{,ii} + P_{i,i} = 0 \quad \text{in } \Omega, \\
 36 \quad \phi_{,ii} = 0 \quad \text{in } \Omega^*, \quad (5a-d)$$

37 where ϕ , \mathbf{E}^0 , \mathbf{F} are the electric potential, external electric field and external force
 38 respectively, t_{ij} , E_i and P_i are the components of the stress tensor, effective local electric
 39 field and the polarization vector respectively while E_{ij} and t_{ijm} represents the higher-order
 40 local electric force and stress, which includes higher-order gradients of the displacement
 41 vector (like $u_{i,jm}$), respectively. Note that these electromechanical stresses are defined as the
 42 partials of Σ with respect to the of respective field vectors as

47 ³Thus, the material is non-piezoelectric.

$$\begin{aligned}
 t_{ij} &\equiv \frac{\partial \Sigma}{\partial e_{ij}}, & t_{ijm} &\equiv \frac{\partial \Sigma}{\partial u_{i,jm}}, \\
 E_{ij} &\equiv \frac{\partial \Sigma}{\partial P_{i,j}}, & E_i &\equiv \frac{\partial \Sigma}{\partial P_i}.
 \end{aligned} \tag{6a-d}$$

Boundary conditions:

$$\begin{aligned}
 n_i \sigma_{ij} &= t_j, \\
 n_i E_{ij} &= 0, \\
 n_i (\llbracket \varepsilon_0 \phi_{,i} \rrbracket + P_i) &= 0
 \end{aligned} \tag{7a-c}$$

\mathbf{n} and \mathbf{t} are the exterior normal unit vector and the surface traction vector, respectively; ε_0 is the dielectric constant and the symbol $\llbracket \]$ denotes the jump across the surface S .

Constitutive relations:

$$\begin{aligned}
 t_{ij} &= [c_{12} \delta_{ij} \delta_{ps} + 2c_{44} \delta_{ip} \delta_{js}] u_{p,s} + [d_{12} \delta_{ij} \delta_{ps} + d_{44} (\delta_{is} \delta_{jp} + \delta_{js} \delta_{ip})] P_{p,s}, \\
 t_{ijm,m} &= [f_{12} \delta_{pi} \delta_{js} + f_{44} (\delta_{ps} \delta_{ji} + \delta_{is} \delta_{jp})] P_{p,s}, \\
 E_{ij} &= [d_{12} \delta_{ij} \delta_{ps} + d_{44} (\delta_{is} \delta_{jp} + \delta_{js} \delta_{ip})] u_{p,s} \\
 &\quad + [b_{12} \delta_{ij} \delta_{ps} + (b_{44} + b_{77}) \delta_{is} \delta_{jp} + (b_{44} - b_{77}) \delta_{js} \delta_{ip}] P_{p,s}, \\
 E_i &= -(a P_i + [f_{12} \delta_{ij} \delta_{ps} + f_{44} (\delta_{is} \delta_{jp} + \delta_{js} \delta_{ip})] u_{j,ps}).
 \end{aligned} \tag{8a-d}$$

Eqs. (8a-d) can be combined with Eqs. (5a-d) to yield the following Navier-like governing equations:

$$\begin{aligned}
 c_{44} \nabla^2 \mathbf{u} + (c_{12} + c_{44}) \nabla \nabla \mathbf{u} + (d_{44} - f_{12}) \nabla^2 \mathbf{P} + (d_{12} + d_{44} - 2f_{44}) \nabla \nabla \mathbf{P} + \mathbf{F} &= 0, \\
 (d_{44} - f_{12}) \nabla^2 \mathbf{u} + (d_{12} + d_{44} - 2f_{44}) \nabla \nabla \mathbf{u} + (b_{44} + b_{77}) \nabla^2 \mathbf{P} \\
 + (b_{12} + b_{44} - b_{77}) \nabla \nabla \mathbf{P} - a \mathbf{P} - \nabla \phi + \mathbf{E}^0 &= 0, \\
 -\varepsilon_0 \nabla^2 \phi + \nabla \mathbf{P} &= 0.
 \end{aligned} \tag{9a-c}$$

It should be noted that the displacement and polarization fields are coupled through the constants \mathbf{d} and \mathbf{f} . Eq. (9a-c) can be rewritten as

$$\begin{aligned}
 C_{ij} u_j + D_{ij} P_j + F_i &= 0, \\
 D_{ij} u_j + B_{ij} P_j - \phi_{,i} + E_i^0 &= 0, \\
 -\varepsilon_0 \phi_{,ii} + P_{i,i} &= 0,
 \end{aligned} \tag{10a-c}$$

where

$$\begin{aligned}
 C_{ji} &= C_{jpis} \nabla_p \nabla_s = [c_{12} \delta_{jp} \delta_{is} + c_{44} (\delta_{ps} \delta_{ij} + \delta_{js} \delta_{ip})] \nabla_p \nabla_s, \\
 D_{ji} &= D_{jpis} \nabla_p \nabla_s = [(d_{12} + d_{44} - 2f_{44}) \delta_{jp} \delta_{is} + (d_{44} - f_{12}) \delta_{ps} \delta_{ij}] \nabla_p \nabla_s, \\
 B_{ji} &= B_{jpis} \nabla_p \nabla_s - a \delta_{ij} = [b_{12} \delta_{jp} \delta_{is} + (b_{44} + b_{77}) \delta_{ps} \delta_{ij} + (b_{44} - b_{77}) \delta_{js} \delta_{ip}] \nabla_p \nabla_s - a \delta_{ij}.
 \end{aligned} \tag{11a-c}$$

These equations may be solved, in analogy with Kelvin's solution in the theory of linearized elasticity by appropriate Green's functions. We can define two sets of Green's functions $\{G_{in}^1, G_{in}^2, \phi_n^f\}$ and $\{G_{in}^3, G_{in}^4, \phi_n^E\}$ corresponding to Eqs. (10a-c) as follows:

$$\begin{aligned}
1 \quad & C_{ji}G_{in}^1(\mathbf{x} - \mathbf{x}') + D_{ji}G_{in}^2(\mathbf{x} - \mathbf{x}') + \delta_{jm}\delta(\mathbf{x} - \mathbf{x}') = 0, \\
3 \quad & D_{ji}G_{in}^1(\mathbf{x} - \mathbf{x}') + B_{ji}G_{in}^2(\mathbf{x} - \mathbf{x}') - \nabla_j\phi_n^f(\mathbf{x} - \mathbf{x}') = 0, \\
& -\varepsilon_0\nabla^2\phi_n^f(\mathbf{x} - \mathbf{x}') + \nabla_iG_{in}^2(\mathbf{x} - \mathbf{x}') = 0, \\
5 \quad & C_{ji}G_{in}^3(\mathbf{x} - \mathbf{x}') + D_{ji}G_{in}^4(\mathbf{x} - \mathbf{x}') = 0, \\
7 \quad & D_{ji}G_{in}^3(\mathbf{x} - \mathbf{x}') + B_{ji}G_{in}^4(\mathbf{x} - \mathbf{x}') - \nabla_j\phi_n^E(\mathbf{x} - \mathbf{x}') + \delta_{jm}\delta(\mathbf{x} - \mathbf{x}') = 0, \\
& -\varepsilon_0\nabla^2\phi_n^E(\mathbf{x} - \mathbf{x}') + \nabla_iG_{in}^4(\mathbf{x} - \mathbf{x}') = 0. \tag{12a-f}
\end{aligned}$$

As evident, the first three equations (12a–c) are the Navier-like equations for the displacement, polarization and the potential fields corresponding to a *unit point force* (denoted by a delta function). Similarly, Eqs. (12d–f) are the governing equations for the displacement, polarization and the potential fields corresponding to a *unit point electrical field*.

In our previous work (Maranganti et al., 2006) we have derived analytical expressions for the Green's functions corresponding to the Lagrangian of Eq. (3) which includes pure strain-gradient terms (coupled by the tensor \mathbf{g}). Neglecting these purely nonlocal terms the Green's functions become

$$\begin{aligned}
19 \quad & 4\pi G_{ij}^{(1)} = \partial_i\partial_j [C^{(01)}R + C^{(11)}I_1 - C^{(12)}I_2] + \delta_{ij}\nabla^2 [C^{(02)}R + C^{(12)}I_2], \\
21 \quad & 4\pi G_{ij}^{(2)} = 4\pi G_{ij}^{(3)} = \partial_i\partial_j [C^{(21)}I_1 + C^{(22)}I_2] - \delta_{ij}\nabla^2 [C^{(22)}I_2], \\
23 \quad & 4\pi G_{ij}^{(4)} = \partial_i\partial_j \left[\frac{I_1}{a + (\varepsilon_0)^{-1}} - \frac{I_2}{a} \right] + \delta_{ij}\nabla^2 \left[\frac{I_2}{a} \right] \tag{13a-c}
\end{aligned}$$

which are same as those derived by Nowacki and Hsieh (1986). The coefficients $C^{(ij)}$ and expression I_a have been defined in Appendix A.

3. Illustrative solutions for centrosymmetric (spherical) and noncentrosymmetric (orthogonal polyhedral) inclusion

Consider an arbitrary shaped *inclusion* with a prescribed stress-free transformation strain $\boldsymbol{\varepsilon}^*$ in its domain (Ω), located in an infinite isotropic medium. Here we follow the convention that the word “inclusion” refers to an embedded region that has the same mechanical and dielectric properties as the surrounding material but with a transformation strain or polarization prescribed within its domain while the word “inhomogeneity” is referred to as an embedded region with material properties differing from the surrounding matrix. Following Eshelby's (1957) well-known formalism, given a uniform transformation strain, the displacement $u_i(\mathbf{x})$ and the polarization field $P_i(\mathbf{x})$ can be written as

$$\begin{aligned}
41 \quad & u_i(\mathbf{x}) = - \int [c_{12}\delta_{jl}\delta_{mn} + 2c_{44}\delta_{jm}\delta_{ln}] \varepsilon_{mnl}^*(\mathbf{x}') G_{ij,l}^1(\mathbf{x} - \mathbf{x}') d\mathbf{x}' \\
43 \quad & - \int [(d_{12} - f_{44})\delta_{jl}\delta_{mn} + (2d_{44} - f_{12} - f_{44})\delta_{jm}\delta_{ln}] \varepsilon_{mnl}^*(\mathbf{x}') G_{ij,l}^2(\mathbf{x} - \mathbf{x}') d\mathbf{x}' \\
45 \quad & \tag{14}
\end{aligned}$$

47 and

$$\begin{aligned}
 P_i(\mathbf{x}) = & - \int [c_{12}\delta_{ji}\delta_{mn} + 2c_{44}\delta_{jm}\delta_{ln}] \varepsilon_{mn}^*(\mathbf{x}') G_{ij,j}^3(\mathbf{x} - \mathbf{x}') d\mathbf{x}' \\
 & - \int [(d_{12} - f_{44})\delta_{ji}\delta_{mn} + (2d_{44} - f_{12} - f_{44})\delta_{jm}\delta_{ln}] \varepsilon_{mn}^*(\mathbf{x}') G_{ij,j}^4(\mathbf{x} - \mathbf{x}') d\mathbf{x}',
 \end{aligned} \quad (15)$$

7 where $\{G_{in}^1, G_{in}^2, G_{in}^3, G_{in}^4\}$ are defined as the set of Green's functions corresponding to Eqs. (12a-f) and are defined in Eqs. (13a-c).

9 Now, for a given transformation strain the polarization P_i for an inclusion of any shape can be written in terms of potentials $\phi(x)$, $\psi(x)$, $M^a(x)$ as

$$\begin{aligned}
 P_i(\mathbf{x}) = & - (3c_{12} + 2c_{44}) \varepsilon^* \partial_i \left(A^{(2)} \phi_{,kk} + C^{(2)} M^1_{,kk} + D^{(2)} M^2_{,kk} \right) \\
 & - [3(d_{12} - f_{12}) + 2(d_{44} - f_{44})] \varepsilon^* \partial_i \left(A^{(3)} \phi_{,kk} + C^{(3)} M^1_{,kk} + D^{(3)} M^2_{,kk} \right), \quad (16)
 \end{aligned}$$

15 where

$$\phi(x) = \frac{1}{4\pi} \int_{\Omega} \frac{1}{R} d\mathbf{x}', \quad \psi(x) = \frac{1}{4\pi} \int_{\Omega} R d\mathbf{x}', \quad M^a(x) = \frac{1}{4\pi} \int_{\Omega} \frac{e^{-R/l_a}}{R} d\mathbf{x}' \quad (17a-c)$$

17 R is $|\mathbf{x} - \mathbf{x}'|$ and l_a are the length scale parameters defined in Appendix A.

21 It is important to note that the inclusion geometry dependence of Eq. (16) is buried within the definitions of the potentials $\phi(x)$, $\psi(x)$ and $M^a(x)$. Thus the solution of the polarization field of an embedded transformed inclusion is reduced entirely to the determination of the three potentials. The first two are merely the Newtonian (i.e. Harmonic) and Biharmonic potential for the inclusion shape while the third is the lesser known and harder to evaluate Yukawa potential. Closed form expressions for the Newtonian and Biharmonic potential exist for a variety of shapes (see for example, Mura, 1987) while only spherical and circular shape is amenable to analytical reduction in the case of Yukawa potential (e.g. Gibbons and Whiting, 1981; Cheng and He, 1997).

29 **Andreev and Downes (1999)**, in connection with quantum dot structures, suggested a general analytical method using Fourier transform technique that allows straightforward separation of shape effects. The characteristic function for the inclusion $\chi(\mathbf{r})$ is defined as

$$\chi(\mathbf{r}) = \begin{cases} 1, & \mathbf{r} \in \Omega, \\ 0, & \mathbf{r} \notin \Omega. \end{cases} \quad (18)$$

37 The Fourier transform of the characteristic function is

$$\hat{\chi}(\mathbf{q}) = \int_{\Omega} e^{-i\mathbf{q}\mathbf{x}} dV(\mathbf{x}). \quad (19)$$

41 The polarization field (Eq. (16)) can be re-written in Fourier space as

$$\widehat{P}_i(\mathbf{q}) = iq_i q_k q_k \hat{\chi}(\mathbf{q}) \varepsilon^* \left\{ \begin{aligned} & \tilde{c} \left(A^{(2)} \widehat{\phi}(\mathbf{q}) + C^{(2)} \widehat{M}^1(\mathbf{q}) + D^{(2)} \widehat{M}^2(\mathbf{q}) \right) \\ & + \tilde{d} \left(A^{(3)} \widehat{\phi}(\mathbf{q}) + C^{(3)} \widehat{M}^1(\mathbf{q}) + D^{(3)} \widehat{M}^2(\mathbf{q}) \right) \end{aligned} \right\}, \quad (20)$$

47 where

$$\tilde{c} = (3c_{12} + 2c_{44}), \quad \tilde{d} = (3(d_{12} - f_{12}) + 2(d_{44} - f_{44})).$$

Thus, substituting Eqs. (17a–c) in Eq. (16) and transforming to Fourier space, we obtain the following analytical expression for the polarization:

$$\widehat{P}_i(\mathbf{q}) = i q_i q_k q_k \hat{\chi}(\mathbf{q}) \varepsilon^* \left(\frac{\tilde{c}A^{(2)} + \tilde{d}A^{(3)}}{q^2} + \frac{\tilde{c}C^{(2)} + \tilde{d}C^{(3)}}{q^2 + (1/l_1^2)} + \frac{\tilde{c}D^{(2)} + \tilde{d}D^{(3)}}{q^2 + (1/l_2^2)} \right), \quad (21)$$

The complete shape information for the inclusion is contained within $\hat{\chi}(\mathbf{q})$ making other terms in Eq. (21) independent of the shape (and geometry) effects. Eq. (21) can now be used to evaluate the polarization field for inclusion of any geometry in Fourier space, if $\hat{\chi}(\mathbf{q})$ for that geometry is known.

For the spherical shape, the shape function has a simple form (Andreev and Downes, 1999)

$$\hat{\chi}(\mathbf{q}, R) = \frac{4\pi}{q} \left(\frac{\sin(\mathbf{q}R)}{q^2} - \frac{R \cos(\mathbf{q}R)}{q^2} \right). \quad (22)$$

Here R is the radius of inclusion. Eq. (21) along with Eq. (22) may then be solved numerically using spectral method (Trefethen, 2000). A periodic distribution ($n_x d, n_y d, n_z d$) of inclusions is used. If a single inclusion solution is desired, a large cell-spacing must be employed to avoid interaction effects while (for eventual composite applications), the spacing may be adjusted to take into account finite volume fraction. Dimension d is normalized with the characteristic length-scale and each unit cell is uniformly meshed. A distribution of polarization field is thus obtained in the Fourier space which is then inverted back to the real space numerically. Thus contour-plots of the normalized electric fields distribution as a function of size and material property combinations (i.e. different combination of the characteristic lengths) for a spherical inclusion under dilatational strain may be obtained. Of course, for spherical geometry, analytical expressions for the potentials are available which can be directly used to generate such contour-plots which are shown here in Fig. 5. The numerical scheme described above is however general and essential for shapes other than spherical or cylindrical.

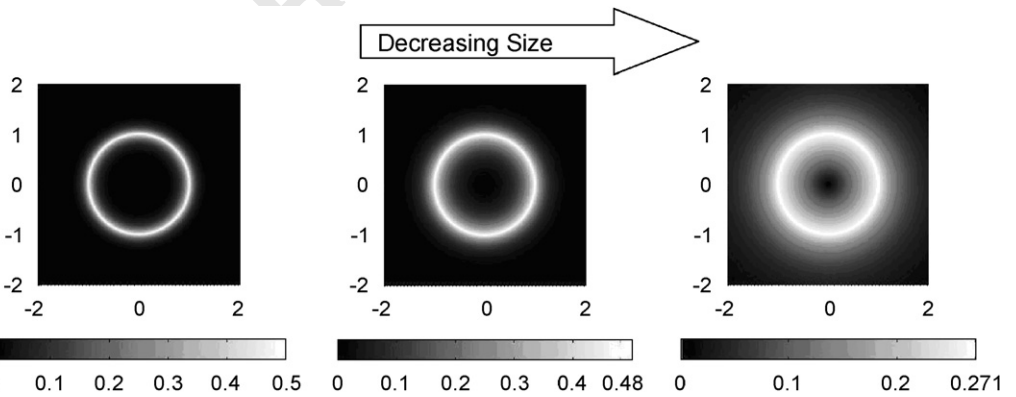


Fig. 5. Normalized contour plots of the electric fields around a spherical inclusion for different sizes subject to dilatational eigenstrain.

1 In Fig. 5, darker regions indicate low concentration of polarization while a lighter shade
 2 indicates a higher concentration of polarization. The material is non-piezoelectric and yet
 3 due to the presence of strain gradients, there exists a finite polarization in and around the
 4 inclusion. As the size increases, the electric field becomes increasingly localized in thinner
 5 and thinner layers at the interface. Unlike the points at the interface, the interior points of
 6 the inclusion exhibit appreciable values only at sizes that are close to the flexoelectric
 7 characteristic length scales. To be more concrete and for illustration, we choose
 8 InAs–GaAs as an example inclusion-matrix system. Both are important quantum dot
 9 materials and subject to a large lattice mismatch induced dilatational transformation
 10 mismatch strain of $\sim 6.7\%$. We then find that for an inclusion size of 5 nm, even far from
 11 the interface (i.e. a distance of $0.1 \times$ radius from center), electric fields of hundreds of kV/m
 12 can be expected (this is in addition to the weakly classical piezoelectric effect in GaAs).
 13 We should mention that spherical and such highly symmetric shapes are *useless* for
 14 obtaining effective piezoelectric coefficients from non-piezoelectric constituents. The high
 15 symmetry of such shapes ensures that the net averaged polarization vanishes globally
 16 although locally it is non-zero. These results are included here to bring about some of the
 17 qualitative nuances of the flexoelectric phenomenon.

As will be proved in Section 4, of real interest to the theme of the manuscript are inclusions of
 18 non-centrosymmetric shape. In Fig. 6 we plot contours of the numerically generated magnitude
 19 of the polarization field for orthogonal polyhedral shaped inclusion (shown in Fig. 4b) subject to
 20 a dilatational transformation strain. Characteristic shape function $\hat{\chi}(\mathbf{q})$ for the orthogonal
 21 polyhedral with a, b, c as the x, y, z -coordinate intercepts, respectively is easily derived to be

$$\hat{\chi}(\mathbf{q}, a, b, c) = \frac{\left(iabe^{-iq_3} q_1 q_2 (aq_1 - bq_2) + iace^{-ibq_2} q_1 q_3 (cq_3 - aq_1) \right) + i bce^{-iaq_1} q_2 q_3 (bq_2 - cq_3) + (aq_1 - bq_2)(bq_2 - cq_3)(cq_3 - aq_1)}{(aq_1 - bq_2)(bq_2 - cq_3)(cq_3 - aq_1)}, \quad (23)$$

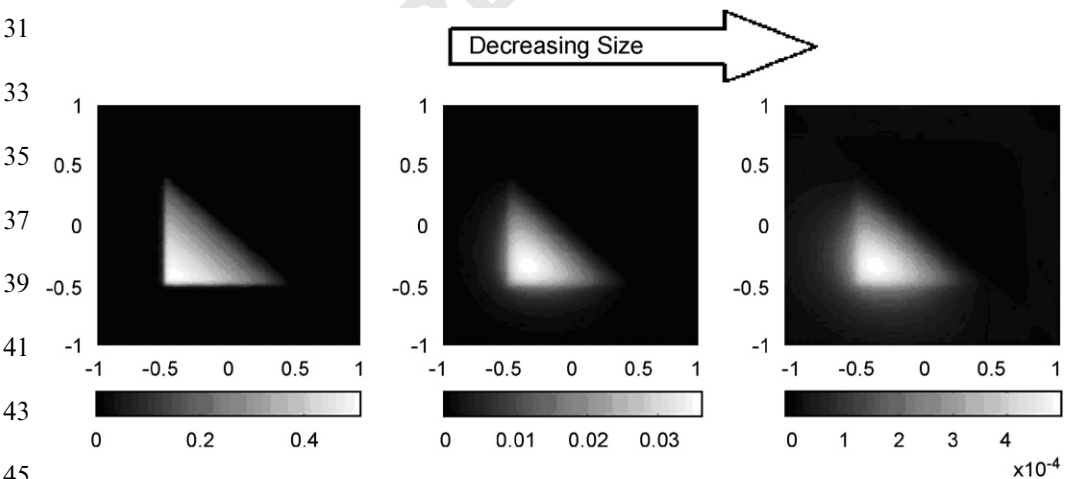


Fig. 6. Normalized contour plots of z -component of polarization around x - y plane of an orthogonal polyhedral inclusion for different sizes.

1 where q_1, q_2, q_3 are the wave vectors.

2 The size effect is evident as in the spherical case. With reduction in size, the electric field
3 is seen to get denser in and around the inclusion. The distribution of the electric field is not
4 symmetric. The *lack of centrosymmetry* in the distribution of polarization field results in a
5 non-zero net averaged polarization in the inclusion (and thus by extension in the whole
6 body). A notable observation is that if the inclusions were to be arranged in a
7 *centrosymmetric topology* (say for example, randomly oriented), the averaged polarization
8 will average to zero over the entire domain. Hence a proper arrangement of such *non-*
9 *centrosymmetric shapes* and a *non-centrosymmetric topology* is necessary to generate non-
10 zero average polarization. In the next section we formally provide this insight based on the
11 mathematical structure of the governing equations.

13 4. Proposition: the requirement of material non-centrosymmetry for piezoelectricity in 14 crystals is transferred to inhomogeneity shape and arrangement in flexoelectric continuum

15 Consider the case of a *centrosymmetric inhomogeneity* embedded inside an infinitely
16 large medium.

17 *Case 1:* Applied voltage boundary condition as specified below exists

$$19 \quad \phi(\mathbf{x})|_{\mathbf{x}=\mathbf{y}} = V, \quad \phi(\mathbf{x})|_{\mathbf{x}=-\mathbf{y}} = -V. \quad (24)$$

21 Since we have a centrosymmetric inhomogeneity, the boundary condition is anti-
22 centrosymmetric in the potential ' $\phi(\mathbf{x})$ '. Thus, the solution of the potential ' $\phi(\mathbf{x})$ ' will
23 exhibit the same anti-centrosymmetry as that exhibited by the boundary condition. Then it
24 follows that the potential ' $\phi(\mathbf{x})$ ' is an odd function in \mathbf{x} :

$$25 \quad \phi(\mathbf{x}) = -\phi(-\mathbf{x}). \quad (25)$$

27 Substituting the above condition in Eq. (9c), we observe that the polarization field must
28 be an even function in ' \mathbf{x} ',⁴ i.e.

$$29 \quad \mathbf{P}(\mathbf{x}) = \mathbf{P}(-\mathbf{x}). \quad (26)$$

31 Further, substituting Eq. (25) into Eq. (9a), we observe that the displacement field ' $\mathbf{u}(\mathbf{x})$ '
32 is also an even function in \mathbf{x} , i.e.

$$33 \quad \mathbf{u}(\mathbf{x}) = \mathbf{u}(-\mathbf{x}). \quad (27)$$

35 As a result of the above symmetry requirement on the displacement field, the strain field
36 ' $\boldsymbol{\varepsilon}(\mathbf{x})$ ' is rendered an odd-function, i.e.

$$37 \quad \boldsymbol{\varepsilon}(\mathbf{x}) = -\boldsymbol{\varepsilon}(-\mathbf{x}). \quad (28)$$

39 Thus the strain averaged over the volume of the system in the case of applied voltage
40 condition is zero.

41 *Case 2:* Traction boundary condition exists as specified below

$$42 \quad \boldsymbol{\sigma}\mathbf{n}|_{\Gamma=S} = \mathbf{t}. \quad (29)$$

43 Once again, since the inhomogeneity is centrosymmetric, the given boundary condition
44 is also centrosymmetric with respect to the stress ' $\boldsymbol{\sigma}(\mathbf{x})$ '. Thus, the solution of the stress
45 function ' $\boldsymbol{\sigma}(\mathbf{x})$ ' is also centrosymmetric. Then it follows that the stress ' $\boldsymbol{\sigma}(\mathbf{x})$ ' is an even

47 ⁴Here we have used the fact that the derivative of an odd function is an even function and vice versa.

1 function in \mathbf{x} . The stress field can be written in terms of the displacement and polarization
fields as

$$\begin{aligned} \sigma_{ij}(\mathbf{x}) = & c_{12}\delta_{ij}u_{k,k}(\mathbf{x}) + c_{44}(u_{i,j}(\mathbf{x}) + u_{j,i}(\mathbf{x})) \\ & + d_{12}\delta_{ij}P_{k,k}(\mathbf{x}) + d_{44}(P_{i,j}(\mathbf{x}) + P_{j,i}(\mathbf{x})). \end{aligned} \quad (30)$$

Since $\boldsymbol{\sigma}(\mathbf{x})$ is even in \mathbf{r} we can infer that

$$\begin{aligned} c_{12}\delta_{ij}u_{k,k}(\mathbf{x}) + c_{44}(u_{i,j}(\mathbf{x}) + u_{j,i}(\mathbf{x})) + d_{12}\delta_{ij}P_{k,k}(\mathbf{x}) + d_{44}(P_{i,j}(\mathbf{x}) + P_{j,i}(\mathbf{x})) \\ = c_{12}\delta_{ij}u_{k,k}(-\mathbf{x}) + c_{44}(u_{i,j}(-\mathbf{x}) + u_{j,i}(-\mathbf{x})) + d_{12}\delta_{ij}P_{k,k}(-\mathbf{x}) \\ + d_{44}(P_{i,j}(-\mathbf{x}) + P_{j,i}(-\mathbf{x})). \end{aligned} \quad (31)$$

From Eq. (9a) we observe that $\mathbf{u}(\mathbf{x})$ and $\mathbf{P}(\mathbf{x})$ have to be either both odd or both even. One can easily verify that if one of them is odd and the other function is even (or vice versa) then Eq. (9a) can never be satisfied. Further, from Eq. (27) we deduce that $\mathbf{u}(\mathbf{x})$ and $\mathbf{P}(\mathbf{x})$ have to be both odd. Since $\mathbf{P}(\mathbf{x})$ is odd, the polarization averaged over the volume of the system becomes zero.

Thus, to obtain effective piezoelectric behavior *without using piezoelectric constituents*, the symmetry of the internal arrangement must be chosen carefully. Any topology that has symmetry of transverse isotropy or less will yield a net overall polarization due to this effect (higher symmetry cannot sustain odd-order tensors that characterize the topology). In other words, *the requirement of material non-centrosymmetry for naturally occurring piezoelectrics is transferred to a requirement of shape/topology non-centrosymmetry in flexoelectric media*. Hence, for example, 2-layer laminate or the conical particle reinforced thin film shown in Fig. 3 are candidates that can demonstrate this effect.

5. Homogenization scheme for apparently piezoelectric composites

In this section we present a simple homogenization scheme that allows us to quantitatively, albeit approximately, estimate the effective piezoelectric behavior of a nanocomposite that is not comprised of piezoelectric materials. Our goal in the present manuscript is to demonstrate this central idea rather than develop a rigorous homogenization theory hence the simplest possible approach is employed.

Consider an infinite non-piezoelectric matrix containing an arbitrary shaped inhomogeneity subject to a far-field uniform strain, $\boldsymbol{\varepsilon}^\infty$. The Navier-like equations (Eqs. (9a–c)) may be re-written in an alternative form as

$$\begin{aligned} \nabla(\mathbf{C} : \boldsymbol{\varepsilon} + \mathbf{D} : \nabla\mathbf{P}) + \mathbf{F} &= 0, \\ \nabla(\mathbf{D} : \boldsymbol{\varepsilon} + \mathbf{B} : \nabla\mathbf{P}) - \nabla\phi + \mathbf{E}^0 &= 0, \\ -\varepsilon_0\nabla^2\phi + \nabla\mathbf{P} &= 0. \end{aligned} \quad (32a-c)$$

We define the position-dependent material properties as

$$\begin{aligned} \mathbf{C}(\mathbf{x}) &= \mathbf{C}^m + (\mathbf{C}^i - \mathbf{C}^m) : \mathbf{H}(\mathbf{x}) \Rightarrow \mathbf{C}^m + [\mathbf{C}] : \mathbf{H}(\mathbf{x}), \\ \mathbf{D}(\mathbf{x}) &= \mathbf{D}^m + [\mathbf{D}] : \mathbf{H}(\mathbf{x}), \\ \mathbf{B}(\mathbf{x}) &= \mathbf{B}^m + [\mathbf{B}] : \mathbf{H}(\mathbf{x}), \end{aligned} \quad (33)$$

where

$$\begin{aligned}
1 \quad & \mathbf{H}(\mathbf{x}) = \begin{cases} \mathbf{1} \dots \mathbf{x} \in V, \\ 3 \quad \mathbf{0} \dots \mathbf{x} \notin V, \end{cases} \\
& \mathbf{C}^m, \mathbf{D}^m, \mathbf{B}^m \rightarrow \text{Material property tensors for matrix,} \\
5 \quad & \mathbf{C}^i, \mathbf{D}^i, \mathbf{B}^i \rightarrow \text{Material Property tensors for the inhomogeneity, and} \\
7 \quad & [] = \text{difference between properties of the matrix and the inhomogeneity.} \quad (34)
\end{aligned}$$

9 Hence Eq. (27a) becomes

$$\begin{aligned}
11 \quad & \nabla\{\mathbf{C}(\mathbf{x}) : \boldsymbol{\varepsilon} + \mathbf{D}(\mathbf{x}) : \nabla\mathbf{P}\} = \mathbf{0} \\
& \Rightarrow \nabla\{\mathbf{C}^m : \boldsymbol{\varepsilon} + [\mathbf{C}] : \boldsymbol{\varepsilon} \mathbf{H}(\mathbf{x}) + \mathbf{D}^m : \nabla\mathbf{P} + [\mathbf{D}] : \mathbf{P} \mathbf{H}(\mathbf{x})\} \\
13 \quad & \Rightarrow \nabla\{\mathbf{C}^m : \boldsymbol{\varepsilon}\} + \nabla\{[\mathbf{C}] : \mathbf{u} \mathbf{H}(\mathbf{x})\} + \nabla\{\mathbf{D}^m : \nabla\mathbf{P}\} + \nabla\{[\mathbf{D}] : \nabla\mathbf{P} \mathbf{H}(\mathbf{x})\} \\
15 \quad & \Rightarrow \nabla\{\mathbf{C}^m : \boldsymbol{\varepsilon} + \mathbf{D}^m : \nabla\mathbf{P}\} + \underbrace{[\mathbf{C}] : \boldsymbol{\varepsilon} \delta(S) + [\mathbf{D}] : \nabla\mathbf{P} \delta(S)}_{=\text{Body Force}} = \mathbf{0}. \quad (35)
\end{aligned}$$

17 Similarly

$$\begin{aligned}
19 \quad & \nabla\{\mathbf{D}(\mathbf{x}) : \boldsymbol{\varepsilon} + \mathbf{B}(\mathbf{x}) : \nabla\mathbf{P}\} = \mathbf{0} \\
21 \quad & \Rightarrow \nabla\{\mathbf{D}^m : \boldsymbol{\varepsilon} + \mathbf{B}^m : \nabla\mathbf{P}\} + \underbrace{[\mathbf{D}] : \boldsymbol{\varepsilon} \delta(S) + [\mathbf{B}] : \nabla\mathbf{P} \delta(S)}_{=\text{Body Electric Field}} = \mathbf{0}. \quad (36)
\end{aligned}$$

23 Thus an inhomogeneity within a matrix can be modeled as a fictitious body force and a
 25 fictitious body electric field. As customary in micromechanics (and already demonstrated
 in Section 3), the displacement \mathbf{u} and polarization \mathbf{P} can be expressed in terms of the
 derived Green's functions as

$$27 \quad \mathbf{u} = \mathbf{u}^\infty - \int_{V'} \mathbf{G}^1 \nabla\{[\mathbf{C}] : \boldsymbol{\varepsilon}(\mathbf{x}')\} dV' - \int_{V'} \mathbf{G}^2 \nabla\{[\mathbf{D}] : \nabla\mathbf{P}(\mathbf{x}')\} dV' \quad (37)$$

29 and

$$31 \quad \mathbf{P}(\mathbf{x}) = \mathbf{P}^\infty - \int_{V'} \mathbf{G}^3 \nabla\{[\mathbf{D}] : \boldsymbol{\varepsilon}(\mathbf{x}')\} dV' - \int_{V'} \mathbf{G}^4 \nabla\{[\mathbf{B}] : \nabla\mathbf{P}(\mathbf{x}')\} dV'. \quad (38)$$

35 Employing Gauss theorem and discarding the boundary terms, we obtain

$$\begin{aligned}
37 \quad & u_i(\mathbf{x}) = u_i^\infty + \int_{V'} \left\{ G_{ji}^1(\mathbf{y}' - \mathbf{x}') \right\}_{,j} \{ [C_{klmn}] \varepsilon_{mn}(\mathbf{x}') \} dV' \\
39 \quad & + \int_{V'} \left\{ G_{ji}^2(\mathbf{y}' - \mathbf{x}') \right\}_{,j} \{ [D_{klmn}] P_{m,n}(\mathbf{x}') \} dV', \quad (39)
\end{aligned}$$

$$\begin{aligned}
41 \quad & P_i(\mathbf{x}) = P_i^\infty + \int_{V'} \left\{ G_{ji}^3(\mathbf{y}' - \mathbf{x}') \right\}_{,j} \{ [D_{jlmn}] \varepsilon_{mn}(\mathbf{x}') \} dV' \\
43 \quad & + \int_{V'} \left\{ G_{ji}^4(\mathbf{y}' - \mathbf{x}') \right\}_{,j} \{ [B_{jlmn}] P_{m,n}(\mathbf{x}') \} dV'. \quad (40)
\end{aligned}$$

47 The strain field is then

$$\begin{aligned} \varepsilon_{ij}(\mathbf{x}) = & \varepsilon_{ij}^{\infty} + \frac{1}{2} \int_{V'} \left\{ G_{jk,li}^1(\mathbf{y}' - \mathbf{x}') + G_{ik,lj}^1(\mathbf{y}' - \mathbf{x}') \right\} \{ [C_{klmn}] \varepsilon_{mn}(\mathbf{x}') \} dV' \\ & + \frac{1}{2} \int_{V'} \left\{ G_{jk,li}^2(\mathbf{y}' - \mathbf{x}') + G_{ik,lj}^2(\mathbf{y}' - \mathbf{x}') \right\} \{ [D_{klmn}] P_{m,n}(\mathbf{x}') \} dV'. \end{aligned} \quad (41)$$

Eqs. (40) and (41) are integral equations that must be solved to determine the polarization and strain states of an unbounded body containing an inhomogeneity under the extended theory of electromechanical coupling that incorporate flexoelectricity. In classical elasticity (for ellipsoidal shape), the strain is uniform within the inhomogeneity and thus allows one to take the strain field out of the integral sign effectively converting the integral equation into an algebraic one. This is not possible in our case as both strain and polarization are inhomogeneous (even for ellipsoidal shape) let alone for non-centrosymmetric shapes that are relevant in the present context. Thus, a suitable approximation must be found to solve Eqs. (40) and (41) and evaluate the average polarization.

A perturbation type approach (cf. Markov, 1979 in the context of micropolar solids) can be used to solve these integral equations. As a first approximation we may assume that the actual strain (polarization field) to be the average uniform strain (polarization field). This approximation is merely the first term in the perturbation series involving the difference between the matrix-inhomogeneity moduli—the next order approximation, as it turns out, was found to be negligible (see Appendix B). Subject to this assumption, Eqs. (41) and (40), respectively, become

$$\begin{aligned} \varepsilon_{ij}(\mathbf{x}) \approx & \varepsilon_{ij}^{\infty} + \frac{1}{2} \int_{V'} \left\{ G_{jk,li}^1(\mathbf{y}' - \mathbf{x}') + G_{ik,lj}^1(\mathbf{y}' - \mathbf{x}') \right\} \{ [C_{klmn}] \langle \varepsilon_{mn} \rangle \} dV' \\ & + \frac{1}{2} \int_{V'} \left\{ G_{jk,li}^2(\mathbf{y}' - \mathbf{x}') + G_{ik,lj}^2(\mathbf{y}' - \mathbf{x}') \right\} \{ [D_{klmn}] \langle P_{m,n} \rangle \} dV', \\ P_i(\mathbf{x}) = & P_i^{\infty} + \int_{V'} G_{ki,l}^3(\mathbf{y}' - \mathbf{x}') [D_{klmn}] \langle \varepsilon_{mn} \rangle dV' + \int_{V'} G_{ki,l}^4(\mathbf{y}' - \mathbf{x}') [B_{klmn}] \langle P_{m,n} \rangle dV'. \end{aligned} \quad (42a-b)$$

Further, taking average values over V on both sides in these equations, we obtain

$$\begin{aligned} \langle \varepsilon_{ij} \rangle \approx & \varepsilon_{ij}^{\infty} + \frac{1}{2} \left\langle \int_{V'} \left\{ G_{jk,li}^1(\mathbf{y}' - \mathbf{x}') + G_{ik,lj}^1(\mathbf{y}' - \mathbf{x}') \right\} dV' \right\rangle [C_{klmn}] \langle \varepsilon_{mn} \rangle \\ & + \frac{1}{2} \left\langle \int_{V'} \left\{ G_{jk,li}^2(\mathbf{y}' - \mathbf{x}') + G_{ik,lj}^2(\mathbf{y}' - \mathbf{x}') \right\} dV' \right\rangle [D_{klmn}] \langle P_{m,n} \rangle, \\ \langle P_i \rangle = & P_i^{\infty} + \left\langle \int_{V'} G_{ki,l}^3(\mathbf{y}' - \mathbf{x}') dV' \right\rangle [D_{klmn}] \langle \varepsilon_{mn} \rangle \\ & + \left\langle \int_{V'} G_{ki,l}^4(\mathbf{y}' - \mathbf{x}') dV' \right\rangle [B_{klmn}] \langle P_{m,n} \rangle. \end{aligned} \quad (43a-b)$$

Further algebraic manipulations lead to following expressions in terms of the material constants, potentials (Eqs. (17a-c)) and the average strains:

$$\langle \varepsilon_{ij} \rangle \approx \varepsilon_{ij}^{\infty} + \left\langle \left\{ \Omega_{iklj}^{(1)} + \frac{\delta_{ik} \Omega_{lj}^{(2)} + \delta_{jk} \Omega_{li}^{(2)}}{2} - \Omega_{iklj}^{(3)} \right\} \right\rangle [C_{klmn}] \langle \varepsilon_{mn} \rangle, \quad (44)$$

47 where

$$\begin{aligned}
1 \quad \Omega_{iklj}^{(1)} &= A^{(1)}\phi_{,iklj} - \frac{B^{(1)}}{2}\psi_{,iklj} + C^{(1)}M_{,iklj}^1 + D^{(1)}M_{,iklj}^2, \\
3 \quad \Omega_{lj}^{(2)} &= E^{(1)}\phi_{,lj} + F^{(1)}M_{,lj}^3 + G^{(1)}M_{,lj}^4, \\
5 \quad \Omega_{iklj}^{(3)} &= \frac{E^{(1)}}{2}\psi_{,iklj} - (F^{(1)}l_3^2 + G^{(1)}l_4^2)\phi_{,iklj} + (F^{(1)}l_3^2M_{,iklj}^3 + G^{(1)}l_4^2M_{,iklj}^4)
\end{aligned}$$

7 and

$$9 \quad \langle P_i \rangle \approx P_i^\infty + \langle \Omega_{kil}^{(4)} + \delta_{ki}\Omega_l^{(5)} - \Omega_{kil}^{(6)} \rangle [D_{klmn}] \langle \varepsilon_{mn} \rangle, \quad (45)$$

11 where

$$\begin{aligned}
13 \quad \Omega_{kil}^{(4)} &= A^{(2)}\phi_{,kil} + C^{(2)}M_{,kil}^1 + D^{(2)}M_{,kil}^2, \\
13 \quad \Omega_l^{(5)} &= F^{(2)}M_{,l}^3 + G^{(2)}M_{,l}^4, \\
15 \quad \Omega_{kil}^{(6)} &= (F^{(2)}l_3^2M_{,kil}^3 + G^{(2)}l_4^2M_{,kil}^4) - (F^{(2)}l_3^2 + G^{(2)}l_4^2)\phi_{,kil}.
\end{aligned}$$

17 Eq. (44) represents a system of six simultaneous algebraic equations in components of $\langle \varepsilon \rangle$ while Eq. (45) provides the three components of polarization field $\langle \mathbf{P} \rangle$.

19 Now, Eqs. (43a–b) involve integration over volume V' of the transformed inclusion. Thus the shape of the inhomogeneity has strong bearing over the polarization and strain fields. As discussed in Section 3, separating the shape effect in the form of a characteristic shape function $\hat{\chi}(\mathbf{q})$ the strain and polarization fields (Eqs. (43a–b)) in Fourier space
21 become

$$\begin{aligned}
25 \quad \langle \widehat{\varepsilon}_{ij} \rangle &\approx \varepsilon_{ij}^\infty - \frac{1}{2} \langle \langle q_l q_i \widehat{G}_{jk}^1 + q_l q_j \widehat{G}_{ik}^1 \rangle \rangle [C_{klmn}] \langle \widehat{\varepsilon}_{mn} \rangle \widehat{\chi}(\mathbf{q}), \\
27 \quad \langle \widehat{P}_i \rangle &\approx P_i^\infty + \langle \langle i q_l \widehat{G}_{ki}^3 \rangle \rangle [D_{klmn}] \langle \widehat{\varepsilon}_{mn} \rangle \widehat{\chi}(\mathbf{q}). \quad (46a-b)
\end{aligned}$$

29 Substituting Eqs. (17a–c) in Eqs. (43a–b), we obtain the following analytical expressions for strain and polarization

$$\begin{aligned}
31 \quad \langle \widehat{\varepsilon} \rangle &\approx (\mathbf{I} - \langle \widehat{\Gamma}^{(1)}(\mathbf{q}) \rangle [\mathbf{C}] \widehat{\chi}(\mathbf{q}))^{-1} \varepsilon^\infty \\
33 \quad \text{and} \\
35 \quad \langle \widehat{\mathbf{P}} \rangle &\approx \mathbf{P}^\infty + \langle \widehat{\Gamma}^{(2)}(\mathbf{q}) \rangle [\mathbf{D}] \langle \widehat{\varepsilon} \rangle \widehat{\chi}(\mathbf{q}). \quad (47a-b)
\end{aligned}$$

37 Here \mathbf{I} is the fourth-order identity tensor and

$$39 \quad \widehat{\Gamma}_{kil}^{(1)}(\mathbf{q}) = q_l q_j \left(-\frac{C^{(11)} q_i q_k}{\mathbf{q}^2 + l_1^2 \mathbf{q}^4} - \frac{2C^{(01)}(-1 + q_i q_k)}{\mathbf{q}^4} + \frac{C^{(12)} - C^{(22)} q_i q_k}{\mathbf{q}^2 + l_2^2 \mathbf{q}^4} \right), \quad (48)$$

$$41 \quad \widehat{\Gamma}_{kil}^{(2)}(\mathbf{q}) = \frac{i q_l (q_k q_i C^{(21)} (1 + l_2^2 \mathbf{q}^2) + (-1 + q_k q_i) C^{(22)} (1 + l_1^2 \mathbf{q}^2))}{\mathbf{q}^2 (1 + l_1^2 \mathbf{q}^2) (1 + l_2^2 \mathbf{q}^2)}. \quad (49)$$

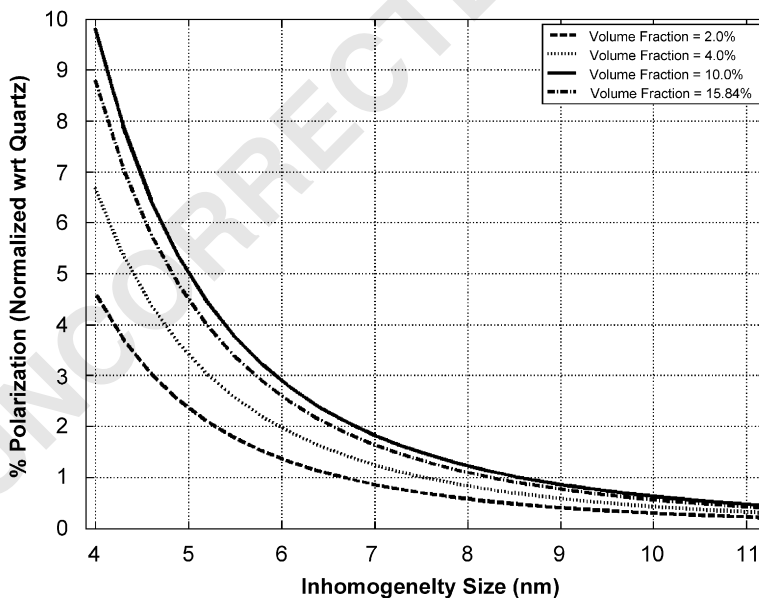
43 Eqs. (47b) along with Eq. (47a) must be solved numerically using spectral method
45 (Trefethen, 2000) as described in Section 3. It is important to note that the unit cell used in the numerical spectral calculations is periodic. The relative sizes of the inhomogeneity and
47 the unit cell define the volume fraction of the composite (e.g. in Fig. 4b, ratio of volume of

1 tetrahedron ($(\frac{1}{6})abc$) to volume of unit cell (a^3) defines the volume fraction). Changing the
 inhomogeneity size for the fixed size of unit-cell allows us to account for various volume
 3 fractions.

5 6. Numerical results

7 The homogenization scheme developed in the previous section is applied to the
 orthogonal polyhedral shape inhomogeneity in Fig. 4b. Currently the availability of
 9 flexoelectric properties for different materials is a major bottleneck. Askar et al. (1970) list
 the isotropic material properties derived from a lattice dynamical model for alkali halides,
 11 in particular NaCl and KCl. Obviously these materials are not the best choice for a
 composite system however our purpose in this work is merely illustrative hence we will
 13 employ properties that correspond to these materials with the caveat that in the future
 (once properties for other dielectric solids have been determined) more practical systems
 15 will be investigated. In principle all dielectric combinations will lead to similar qualitative
 results. Currently efforts are in progress to evaluate flexoelectric material properties via
 17 quantum mechanical Berry phase calculations for various technologically relevant
 dielectrics.

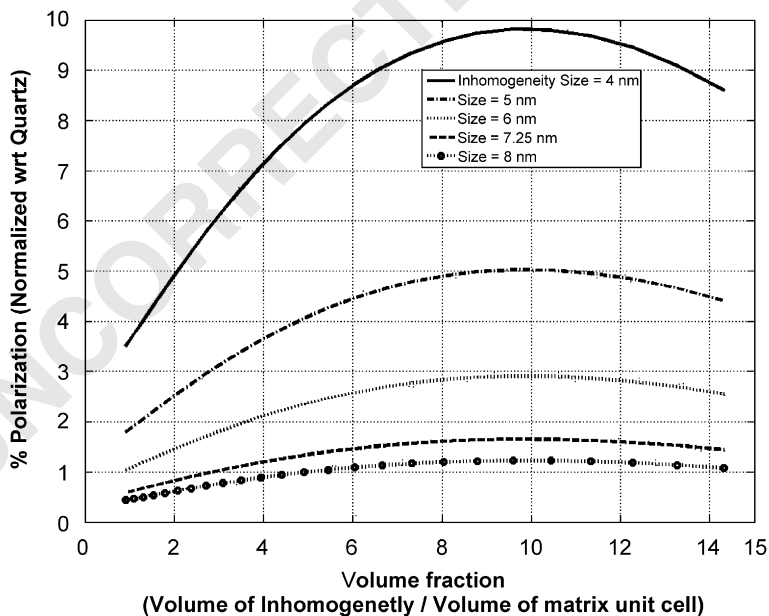
19 Numerically calculated values for the z -component of the polarization (normalized with
 respect to quartz) for different volume fractions are shown in Fig. 7 as a function of the
 21 inhomogeneity size. Inhomogeneity size is indicated by the dimension of one of the sides of
 tetrahedron. As expected, the average polarization vanishes as the size of the
 23 inhomogeneity is increased (corresponding to smaller and smaller strain gradients).



45 Fig. 7. The z -component of the polarization (normalized with respect to quartz) as a function of inclusion size for
 a tetrahedral inhomogeneity depicted in Fig. 4(b). Note that amongst the four different volume fractions
 47 considered (2.0%, 4.0%, 10.0% and 15.84%), maximum polarization is observed for a volume fraction of 10%.

1 Qualitatively, the following can be inferred: assume that the volume fraction of the
 2 second phase is negligibly small. Then, the average strain gradients will also be small and
 3 one will obtain negligible overall piezoelectric behavior. Now consider the other extreme:
 4 the volume fraction is very high. Once again, due to large fraction of one phase, strain state
 5 will become increasingly homogeneous and overall electromechanical coupling will once
 6 again be small. Thus it can be expected that the induced polarization be extremely small for
 7 low concentrations of either of the constituents while it will increase and reach a maximum
 8 at some intermediate volume fraction. This simple qualitative argument alludes to the fact
 9 that for a given topology arrangement and material combination there exists an
 10 “*optimum*” volume fraction for which a maximal overall electromechanical coupling will
 11 be observed. The effect of the volume fraction on the z -component of polarization is
 12 explicitly shown in Fig. 8. We note that for the given inhomogeneity, the maximum
 13 allowed volume fraction is 16.67%, at which the inhomogeneity edge is of the same length
 14 as that of the matrix unit cell. This opens up the prospects for search of optimum size of
 15 the inclusion and the optimum volume fraction of the composite.

16 Given the properties we have chosen—see Appendix A, due to low elastic and dielectric
 17 contrast and relatively low flexoelectric coefficients a maximum of 10% of Quartz
 18 polarization is achieved. Considering that solely non-piezoelectric materials are used, these
 19 numbers are tantalizing and may be easily improved upon (and calculated using the
 20 developed model in our paper) for other materials.



21
22
23
24
25
26
27
28
29
30
31
32
33
34
35
36
37
38
39
40
41
42
43
44
45
46
47 Fig. 8. The z -component of the polarization (normalized with respect to quartz) as a function of volume fraction of the composite with tetrahedral inhomogeneity of non-piezoelectric material in non-piezoelectric matrix.

7. Conclusion and summary

In summary, the universal strain gradient—polarization coupling also known as flexoelectricity—may be employed to create apparently piezoelectric nanocomposites without using piezoelectric materials. Even for a rather poor choice of materials (due to limited data availability) we find that close to 10% of Quartz electromechanical performance can be obtained in the size regime of 4–5 nm. We expect that future work will focus on evaluation of the flexoelectric coefficients of various technologically relevant dielectrics and consequently optimum design of a new class of piezoelectric meta-materials. Currently the authors are attempting to use Berry-phase quantum mechanical approach to evaluate the flexoelectric coefficients and will be reported in future publications. On the theoretical side, there is a need for the further development of rigorous homogenization schemes for the new classes of coupled electromechanical equations discussed in the present work.

Uncited references

Buchanan et al. (1990), Chowdhury and Glockner (1977), Kleinert (1989), Meyer (1969), Nowaki and Hsieh (1986), Nye (1985), Torquato et al. (2002), Torquato and Hyun (2002).

Acknowledgments

Discussions with Xinyuan Zhang are gratefully acknowledged. PS and RM acknowledge support from Office of Naval Research while support for NDS is provided by Texas ARP.

Appendix A

The coefficients $C^{(ij)}$ in the Green's functions defined in Eqs. (13a–c) are:

$$\begin{aligned} C^{(01)} &= \frac{c_{44} + c_{12}}{2c_{44}(c_{12} + 2c_{44})}, & C^{(02)} &= \frac{1}{2c_{44}}, & C^{(11)} &= \frac{d_{11}^2}{(a + \varepsilon_0^{-1})c_{11}^2}, \\ C^{(12)} &= \frac{d_{44}^2}{ac_{44}^2}, & C^{(21)} &= -\frac{d_{11}}{(a + \varepsilon_0^{-1})c_{11}}, & C^{(21)} &= \frac{d_{44}}{ac_{44}} \end{aligned} \quad (\text{A.1})$$

while

$$I_a = \frac{(\exp(-R/l_a) - 1)}{R}. \quad (\text{A.2})$$

In the above equation l_1 and l_2 are new length scale parameters which are defined in terms of the material coefficients as

$$l_1^2 = \frac{b_{11} - (d_{11} - f_{11})^2}{c_{11}(a + \varepsilon_0^{-1})}, \quad l_2^2 = \frac{(b_{44} + b_{77}) - (d_{44} - f_{12})^2}{a}. \quad (\text{A.3})$$

Material Constants for NaCl and KCl are (Askar et al., 1971):

		NaCl	KCl
3	c_{12}	10^{12} dyn/cm ²	0.148
5	c_{44}		0.149
	d_{12}	10^7 dyn-cm/C	0.470
7	d_{44}		-0.170
	b_{12}	10^4 dyn-cm ⁴ /C ²	-1.6×10^{-7}
9	b_{44}		0.344
	b_{77}		0.344
11	a	10^{19} dyn-cm ² /C ²	1.74
	l_1^2	10^{-16} cm ²	0.527
13	c_{44}		3.943
			4.926

15

17 and

$$19 \quad c_{11} = c_{12} + 2c_{44}, \quad d_{11} = d_{12} + 2d_{44}, \quad b_{11} = b_{12} + 2b_{44}.$$

21 Appendix B. Higher-order approximation for $\boldsymbol{\varepsilon}(\mathbf{x}')$

23 We assumed $\boldsymbol{\varepsilon}(\mathbf{x}')$ and $\mathbf{P}(\mathbf{x}')$ to be constant within the inhomogeneity so that $\boldsymbol{\varepsilon}(\mathbf{x}') = \langle \boldsymbol{\varepsilon} \rangle$
 25 and $\mathbf{P}(\mathbf{x}') = \langle \mathbf{P} \rangle$. This is the first-order approximation. A series expansion of the strain
 field can be a better approximation. Let

$$27 \quad \varepsilon_{ij}(\mathbf{x}') = \langle \varepsilon_{ij} \rangle + {}^e a_{ijk} x'_k + {}^e b_{ijkl} x'_k x'_l + \dots,$$

$$29 \quad P_{ij}(\mathbf{x}') = \langle P_{ij} \rangle + {}^p a_{ijk} x'_k + {}^p b_{ijkl} x'_k x'_l + \dots, \quad (\text{B.1})$$

31 where ${}^e a_{ijk}$, ${}^p a_{ijk}$, ${}^e b_{ijkl}$, ${}^p b_{ijkl}$, ... are constants to be determined by solving following
 algebraic equations: Choosing up to second term, we can write Eqs. (41) and (40),
 33 respectively, as

$$35 \quad \varepsilon_{ij}(\mathbf{x}) \approx \varepsilon_{ij}^\infty + \frac{1}{2} \int_{V'} \left\{ G_{jk,li}^1(\mathbf{y}' - \mathbf{x}') + G_{ik,lj}^1(\mathbf{y}' - \mathbf{x}') \right\} \{ [C_{klmn}] (\langle \varepsilon_{mn} \rangle + {}^e a_{ijk} x'_k) \} dV'$$

$$37 \quad + \frac{1}{2} \int_{V'} \left\{ G_{jk,li}^2(\mathbf{y}' - \mathbf{x}') + G_{ik,lj}^2(\mathbf{y}' - \mathbf{x}') \right\} \{ [D_{klmn}] (\langle P_{m,n} \rangle + {}^p a_{ijk} x'_k) \} dV',$$

$$39 \quad P_i(\mathbf{x}) \approx P_i^\infty + \int_{V'} G_{ki,l}^3(\mathbf{y}' - \mathbf{x}') [D_{klmn}] (\langle \varepsilon_{mn} \rangle + {}^e a_{ijk} x'_k) dV'$$

$$41 \quad + \int_{V'} G_{ki,l}^4(\mathbf{y}' - \mathbf{x}') [B_{klmn}] (\langle P_{m,n} \rangle + {}^p a_{ijk} x'_k) dV'. \quad (\text{B.2})$$

43

The polarization field with this higher-order approximation can be calculated following
 45 the same approach as described in Section 5. Our numerical analysis for the second-order
 approximation shows that only a minor improvement is obtained for the given material
 47 properties. This conclusion may change if the elastic or dielectric contrast is large.

1 **References**

- 3 Andreev, A.D., Downes, J.R., 1999. Strain distributions in quantum dots of arbitrary shape. *J. Appl. Phys.* 86, 297–305.
- 5 Askar, A., Lee, P.C.Y., Cakmak, A.S., 1970. Lattice dynamics approach to the theory of elastic dielectrics with polarization gradients. *Phys. Rev. B* 1, 3525–3527.
- 7 Askar, A., Lee, P.C.Y., Cakmak, A.S., 1971. The effect of surface curvature and discontinuity on the surface energy density and other induced fields in elastic dielectrics. *Int. J. Solids Struct.* 7, 523–537.
- 9 Askar, A., Lee, P.C.Y., 1974. Lattice dynamics approach to the theory of diatomic elastic dielectrics. *Phys. Rev. B* 9 (12), 5291–5299.
- 11 Bauer, C.L., Brantley, W.A., 1970. Effect of charged dislocations on a.c. dielectric and elastic properties. *Mater. Sci. Eng.* 5, 295–297.
- 13 Bursian, E.V., Trunov, N.N., 1974. Nonlocal piezoelectric effect. *Fiz. Tverd. Tela* 16, 1187–1190.
- 15 Buchanan, G.R., Sallah, M., Fong, K.F., 1990. Variational principles and finite element analysis for polarization gradient theory. *Comput. Mech.* 5, 447–458.
- 17 Catalan, G., Sinnamoni, L.J., Gregg, J.M., 2004. The effect of flexoelectricity on the dielectric properties of inhomogeneously strained ferroelectric thin films. *J. Phys. Condens. Matter* 16, 2253–2264.
- 19 Cheng, Z.Q., He, L.H., 1997. Micropolar elastic fields due to a spherical inclusion. *Int. J. Eng. Sci.* 33, 389–397.
- 21 Chowdhury, K.L., Glockner, P.G., 1977. On thermoelastic dielectrics. *Int. J. Solids Struct.* 13, 1173–1182.
- 23 Cochran, W., Cowley, R.A., 1962. Dielectric constants and lattice vibrations. *Phys. Chem. Solids* 23, 447–450.
- 25 Cross, L.E., 2006. Flexoelectric effects: charge separation in insulating solids subjected to elastic strain gradients. *J. Mater. Sci.* 41, 53–63.
- 27 Dick, B.J., Overhauser, A.W., 1958. Theory of the dielectric constants of alkali halide crystals. *Phys. Rev.* 112, 90–103.
- 29 Dumitrica, T., Landis, C.M., Yakobson, B.I., 2002. Curvature induced polarization in carbon nanoshells. *Chem. Phys. Lett.* 360, 182–188.
- 31 Eshelby, J.D., 1957. The determination of the elastic field of an ellipsoidal inclusion, and related problems. *Proc. R. Soc. London A* 241, 376–396.
- 33 Fousek, J., Cross, L.E., Litvin, D.B., 1999. Possible piezoelectric composites based on flexoelectric effect. *Mater. Lett.* 39, 289–291.
- 35 Gibbons, G.W., Whiting, B.F., 1981. Newtonian gravity measurements impose constraints on unification theories. *Nature* 291, 636–638.
- 37 Indenbom, V.L., Loginov, V.B., Osipov, M.A., 1981. Flexoelectric effect and structure of crystals. *Kristallografiya* 28, 1157–1162.
- 39 Kleinert, H., 1989. *Gauge Fields in Condensed Matter, Vol. II, Stresses and Defects*. World Scientific, Singapore.
- 41 Kogan, Sh.M., 1963. Piezoelectric effect under an inhomogeneous strain and acoustic scattering of carriers in crystals. *Fiz. Tverd. Tela* 5 (10), 2829–2831.
- 43 Ma, W., Cross, L.E., 2001a. Observation of the flexoelectric effect in relaxor $\text{Pb}(\text{Mg}_{1/3}\text{Nb}_{2/3})\text{O}_3$ ceramics. *Appl. Phys. Lett.* 78 (19), 2920–2921.
- 45 Ma, W., Cross, L.E., 2001b. Large flexoelectric polarization in ceramic lead magnesium niobate. *Appl. Phys. Lett.* 79 (19), 4420–4422.
- 47 Ma, W., Cross, L.E., 2002. Flexoelectric polarization in barium strontium titanate in the paraelectric state. *Appl. Phys. Lett.* 81 (19), 3440–3442.
- 49 Ma, W., Cross, L.E., 2003. Strain-gradient induced electric polarization in lead zirconate titanate ceramics. *Appl. Phys. Lett.* 82 (19), 3923–3925.
- 51 Maranganti, R., Sharma, N.D., Sharma, P., 2006. Electromechanical coupling in nonpiezoelectric materials due to nanoscale nonlocal size effects: Green's function solutions and embedded inclusions. *Phys. Rev. B* 74, 014110-1–014110-14.
- 53 Markov, K., 1979. On the inhomogeneity problem in micropolar elasticity. *Theor. Appl. Mech.* 3, 52–59.
- 55 Marvan, M., Havranek, A., 1988. Flexoelectric effect in elastomers. *Prog. Colloid Polym. Sci.* 78, 33–36.
- 57 Marvan, M., Havranek, A., 1997. Static volume flexoelectric effect in a model of linear chains. *Solid State Commun.* 101 (7), 493–496.
- 59 Maugin, G.A., 1988. *Continuum Mechanics of Electromagnetic Solids*. North-Holland, Amsterdam.
- 61 Meyer, R.B., 1969. Piezoelectric effects in liquid crystals. *Phys. Rev. Lett.* 22, 918–921.
- 63 Mindlin, R.D., 1968. Polarization gradient in elastic dielectrics. *Int. J. Solids Struct.* 4, 637–642.

- 1 Mura, T., 1987. *Micromechanics of Defects in Solids*. Martinus Nijhoff, Hague, The Netherlands.
- 2 Nakhmanson, S.M., Calzolari, A., Meunier, V., Bernholc, J., Nardelli, M.B., 2003. Spontaneous polarization and
3 piezoelectricity in boron nitride nanotubes. *Phys. Rev. B* 67, 235406–235410.
- 4 Nowaki, J.P., Hsieh, R.K.T., 1986. Lattice defects in linear isotropic dielectrics. *Int. J. Eng. Sci.* 24 (10),
5 1655–1666.
- 6 Nowick, A.S., Heller, W.R., 1965. Dielectric and anelastic relaxation of crystals containing point defects. *Adv.*
7 *Phys. (Suppl. Philos. Mag.)* 14 (54), 101–166.
- 8 Nye, J.F., 1985. *Physical Properties of Crystals: Their Representation by Tensors and Matrices*, reprint ed.
9 Oxford University Press, Oxford.
- 10 Robinson, W.H., Glover, A.J., Wolfenden, A., 1978. Electrical–mechanical coupling of dislocations in KCl,
11 NaCl, LiF, and CaF₂. *Phys. Stat. Sol. (a)* 48, 155–163.
- 12 Sahin, E., Dost, S., 1988. A strain-gradient theory of elastic dielectrics with spatial dispersion. *Int. J. Eng. Sci.* 26
13 (13), 1231–1245.
- 14 Schmidt, D., Schadt, M., Helfrich, W., 1972. Liquid-crystalline curvature electricity: the bending mode of MBBA.
15 *Z. Naturforsch. A* 27a (2), 277–280.
- 16 Sharma, P., Ganti, S., Bhate, N., 2003. The effect of surfaces on the size- dependent elastic state of (nano)
17 inhomogeneities. *Appl. Phys. Lett.* 82 (4), 535–537.
- 18 Tagantsev, A.K., 1986. Piezoelectricity and flexoelectricity in crystalline dielectrics. *Phys. Rev. B* 34 (8),
19 5883–5889.
- 20 Tagantsev, A.K., 1991. Electric polarization in crystals and its response to thermal and elastic perturbations.
21 *Phase Transit.* 35 (3–4), 119–203.
- 22 Tolpygo, K.B., 1962. Investigation of long-wavelength vibrations of diamond-type crystals with an allowance for
23 long-range forces. *Sov. Phys.—Solid States* 4 (7), 1765–1777.
- 24 Torquato, S., Hyun, S., 2002. Optimal and manufacturable two-dimensional, Kagome-like cellular solids. *J.*
25 *Mater. Res.* 17 (1), 137–144.
- 26 Torquato, S., Hyun, S., Donev, A., 2002. Multifunctional composites: optimizing microstructures for
27 simultaneous transport of heat and electricity. *Phys. Rev. Lett.* 89 (26), 266601.
- 28 Trefethen, L.N., 2000. *Spectral Methods in Matlab*. SIAM, Philadelphia.
- 29 Whitworth, R.W., 1964. Production of electrostatic potential differences in sodium chloride crystals by plastic
30 compression and bending. *Philos. Mag.* 4 (107), 801–816.
- 31 Zhang, X., Sharma, P., 2005a. Inclusions and inhomogeneities in strain gradient elasticity with couple stresses and
related problems. *Int. J. Solids Struct.* 42, 3833–3851.
- Zhang, X., Sharma, P., 2005b. Size dependency of strain in arbitrary shaped, anisotropic embedded quantum dots
due to nonlocal dispersive effects. *Phys. Rev. B* 72, 195345-1–195345-16.
- Zheludev, I.S., Likhacheva, Y.U.S., Lileeva, N.A., 1969. Further contribution to the question of the electrical
polarization of crystals by torsional deformation. *Kristallografiya* 14 (3), 514–516.
- Zhu, W., Fu, J.Y., Li, N., Cross, L.E., 2006. Piezoelectric composite based on the enhanced flexoelectric effects.
Appl. Phys. Lett. 89, 192904.